

Factors influencing development of cracking-sliding failures of loess across the east Loess Plateau of China

Yanrong Li¹, Jiarui Mao², Xiqiong Xiang², Ping Mo¹

¹Department of Earth Sciences and Engineering, Taiyuan University of Technology, Taiyuan, 030024, China

²Guizhou University, Guiyang, 550025, China

Correspondence to: Yanrong Li (li.dennis@hotmail.com) & Xiqiong Xiang (tujia@126.com)

Abstract: Loess is a porous, weakly cemented, and unsaturated Quaternary sediment deposited by the wind in arid and semiarid regions. Loess is widely and thickly distributed in China, making the Loess Plateau the largest bulk accumulation of loess on Earth. However, the fragile geoenvironment in the loess areas of China causes frequent and various geohazards, such as cracking–sliding failure (“beng-hua” in Chinese), which is a typical mode that causes the largest number of casualties each year. This study investigates the main influencing factors and development patterns of cracking–sliding failure of loess to help prevent its occurrence and reduce losses effectively. The following conclusions are derived: (1) cracking–sliding failures mostly take place in rectilinear slopes, convex slopes, slopes with gradients greater than 60°, slopes with heights of 5 m to 40 m, and sunward slopes with aspects of 180° to 270°; (2) cracking–sliding failures occur mostly from 10 pm to 4 am and mainly in the rainy season (July to September) and in the freeze–thaw season (March to April); and (3) highly intense human activities in the region correspond to a high possibility of cracking–sliding failures.

Keywords: loess, cracking–sliding failure, influencing factors, development patterns

1 Introduction

Any yellowish, carbonate-bearing, quartz-rich, silt-dominated strata formed by aeolian deposition and aggregated by loessification during glacial times are widely accepted as loess (Sprafke and Obreht, 2016). Loess (“huang-tu” in Chinese) and its related deposits are one of the most widespread Quaternary sedimentary formations, and they are most abundant in arid or semiarid regions in inner Eurasia and North America; they are characterized by high porosity, weak cementation, and unsaturation (Samllley et al., 2011).

The Loess Plateau in China (LPC) are the main regions for comprehensive development of agriculture, forestry, animal husbandry, and industrial resources with an arable land area of 173,000 km², which accounts for more than one-fifth of the entire arable land of the country and feed more than 200 million people (Zhang, 2014). However, geohazards, such as

33 cracking–sliding, toppling, falling, sliding, peeling, and caving failures, occur frequently because
34 of fragile geological and natural environments, excessive reclamation, and unreasonable
35 engineering activities. Among these geohazards, cracking–sliding failure, normally with a
36 volume of several hundred cubic meters, causes the largest number of casualties in the east of
37 LPC (Lei, 2001). More than 1000 cracking–sliding failures were recorded in the past two
38 decades, and they caused an average of more than 100 fatalities per year despite the small
39 volumes of individual failures. Unlike “flows” or “slides” as defined by Cruden and Varnes
40 (1996), cracking–sliding failures have composite failure planes composed of two parts. The
41 upper part normally develops vertically from the crown of the slope down to one to several
42 meters deep. The upper part forms by tensile cracking, but the slope can stand stably for a long
43 time with such cracks. The lower part is generally inclined at an angle ranging from 15° to 60°.
44 Sliding along the lower part, which is triggered by rainfall, freezing–thawing, daily temperature
45 fluctuations, slope undercutting, and earth tremors likely mobilizes cracking–sliding failures.

46 According to historical records, 62 cracking–sliding failures occurred in Shenmu, Mizhi,
47 Zizhou, and other places in Northern Shaanxi Province from 1985 to 1993 and caused 258 deaths
48 and more than 40 injuries (Qu et al., 2001). In 2005, the cracking–sliding failure in Jixian County
49 in Shanxi Province resulted in 24 deaths and economic losses of approximately RMB 10 million.
50 Failure with a volume of $2.5 \times 10^4 \text{ m}^3$ took place in Zhongyang County in Shanxi on November
51 16, 2009, causing 23 deaths and destroying 6 houses. In 2013, 36 loess failures were documented
52 in Tianshui City, Gansu Province (Xin et al., 2013). In 2015, a cracking–sliding failure in
53 Linxian County, Shanxi buried four families comprising nine people. All of these failures
54 developed within the loess–paleosol sequence, with relatively uniform mineralogical and
55 chemical compositions. More recently, a cracking-sliding failure occurred in Shilou County of
56 Shanxi Province on March 10, 2018, and destroyed 36 houses (Fig. 1). The original loess slope
57 was characterized by slope gradient of 60°, height of 50 m and aspect of 280°. The scarp of this
58 failure was dominated by near-vertical tensile cracks with an average gradient of 85°. The
59 displaced mass reached 7600 m³.

60 Frequent and disastrous events demand an in-depth understanding of causative factors and
61 development patterns of loess failures to reduce the occurrence of such geohazards. This study
62 collects a large set of data on loess cracking–sliding failures, climate, and soil temperature to
63 facilitate a detailed analysis of the internal and external causes of such failures. This study also
64 emphasizes the influences of slope features (i.e., slope type, gradient, height, and aspect), rainfall,
65 freezing–thawing cycles, daily temperature fluctuations, and human engineering activities.

66 2 Study area

67 The study area is limited to the east of the LPC covering the regions of Northern Shaanxi and
68 Western Shanxi provinces because of their homogeneous background of climatic, morphologic,

69 geologic, and anthropic conditions (Fig. 2). The latitude of the study area ranges from 800 m to
70 1300 m above sea level from southeast to northwest. The study area has a typical semiarid
71 continental monsoon climate with four distinct seasons. The average annual rainfall in this area
72 varies from 400 mm to 700 mm. Rainfall in summer (from July to September) accounts for
73 approximately 70% of the year (Hui, 2010; Qian, 2011; Zhu 2014). For instance, the maximum
74 precipitation in an hour in Yan'an City can accumulate to more than 60 mm in summer (Zhu,
75 2014). The total rainfall in Shilou County reached 412 mm in a month from early July to early
76 August in 2013 (Lv, 2011) and corresponded to 81% of rainfall in the same year. According to
77 records for the past 10 years, the average annual temperature is relatively constant, ranging from
78 8 °C to 12 °C. However, variations in temperature in a day can occasionally be greater than
79 25 °C, that is, the highest temperature is recorded at noon and the lowest temperature is observed
80 at midnight.

81 The study area is located in the east of the Ordos basin. The Fenwei Graben, spanning
82 northeast to southwest, is a subsided area encountering a number of normal and strike-slip faults
83 and covering more than 20,000 km² (Huang et al., 2008; Liu et al., 2013). The thickly bedded
84 Pleistocene loess-paleosol sequence constitutes more than 70% of the study area and reaches a
85 maximum thickness of 300 m. From top to bottom, the loess-paleosol sequence includes Late
86 Pleistocene Malan Loess (Q₃), Middle Pleistocene Lishi Loess (Q₂), and Early Pleistocene
87 Wucheng Loess (Q₁). The Malan Loess, with thickness ranging from 10 m to 30 m, is the most
88 widespread. The Lishi Loess, with several interlayers to tens of interlayers of loess and paleosol,
89 underlies the Malan Loess and forms a 60–150 m thick layer. The Wucheng Loess is
90 sporadically exposed along some loess gullies. Remarkable landforms, such as loess platforms,
91 ridges, and hillocks, have been formed in the study area because of intensive surficial erosion
92 (Zhang, 1983; Zhang, 1986). Loess platforms are mainly distributed in the Luochuan area in
93 Northern Shaanxi Province; loess ridges are mainly found in the peripheries of the Luochuan
94 platform and eastern regions of the Yellow River; and loess hillocks are mainly located in
95 Yan'an, Suide and in both sides of the Yellow River between Shaanxi and Shanxi provinces.

96 **3 Dataset**

97 A large set of data of loess cracking-sliding failure events were collected from published
98 literature and unpublished reports to local governments. Slope profile, gradient, height and
99 aspect, were derived in polygon from the initiation areas. The initiation areas rather than the
100 whole landslides were compared in the following statistical analysis. The polygons were
101 obtained by means of 1) interpretation of remote sensing images which were taken prior to the
102 event; 2) engineering drawings if the host slope was engineered; or 3) post-event field survey
103 and consultation with the local populace. The field survey was normally conducted within 1–2
104 days immediately after each event. A total of 1176 cracking-sliding events were recorded in the
105 past 20 years across the study area. Of these events, 321 were published in the literature, 670

106 were presented in government reports, and 185 were unpublished by the local government. All of
107 the 1176 failures were individually reviewed by verifying the reliability, accuracy, and
108 completeness of the original records. Finally, 458 cases (red dots in Fig. 2) were selected to set
109 up the dataset for this study.

110 Data pertaining to rainfall were obtained from the records of 75 meteorological stations (blue
111 dots in Fig. 2), which are almost uniformly distributed across the study area. Statistical analysis
112 shows that the variation in average annual rainfall in the past 15 years among these stations is
113 less than 80 mm, indicating a relatively homogeneous climatic condition over the study area.

114 **4 Results and discussion**

115 **4.1 Internal factors**

116 Loess slopes are divided into four types in terms of slope profile: rectilinear, convex, concave,
117 and stepped slopes (Table 1). Concave and stepped slopes are more stable than rectilinear and
118 convex slopes. We surveyed 212 loess slopes in Lishi City in Shanxi Province and found that
119 stepped slopes, convex slopes, rectilinear slopes, and concave slopes account for 38%, 31%, 18%,
120 and 13% of all of the slopes, respectively (Fig. 3a). This finding is consistent with the conclusion
121 of Qin et al. (2015), who performed a field survey on loess slopes in Yan'an City, Shaanxi
122 Province. However, approximately one-half of cracking–sliding failures occur in rectilinear
123 slopes. In Fig. 3b, the statistical analysis of the 458 failure cases indicates that rectilinear slopes
124 are the most susceptible to cracking–sliding failure (48%), followed by convex slopes (28%).
125 Stepped (13%) and concave (11%) slopes are the least susceptible to such failures.

126 In general, the overall gradients of rectilinear and convex slopes are steep, resulting in large
127 internal stresses and stress concentrations, particularly at the shoulder and toe sections (Table 1).
128 The bottom part of the concave slope has a gentle gradient and has a supporting function to the
129 steep upper part, thereby relieving the stress concentration; the maximum shear stress at the foot
130 of concave slopes is typically only one-half of the shear stress at the foot of rectilinear slopes
131 (Zhang et al., 2009). The stress distribution pattern in each step section of a stepped slope is
132 similar to that of a rectilinear slope. However, the magnitude of internal stress of stepped slopes
133 is less than that of rectilinear slopes because of the small height of each step and the gentle
134 overall gradient. These findings explain that most cracking–sliding failures occur in rectilinear
135 slopes, although these slopes are not the dominant slope type in the loess area.

136 In addition to slope profile, the gradient, height, and aspect of loess slopes are closely related
137 to the occurrence of cracking–sliding failures. Fig. 4a shows that failure occurs mostly on slopes
138 with gradients greater than 60° and that the number of failures increases with gradients. Of the
139 cracking–sliding failures, 16%, 25%, and 47% occur on slopes with gradients ranging from 61°
140 to 70° , from 71° to 80° , and from 81° to 90° , respectively. Fig. 5 shows the tension zones that

141 developed at slope shoulders, where radial and tangential stresses transform into tensile stresses.
142 The steeper the slope is, the wider the tension band is (Stacey, 1970; Zhang et al., 2009).

143 **Fig. 4b** illustrates that slope height is another main factor that controls the occurrence of
144 cracking–sliding failures. In the study area, most cracking–sliding failures occur on slopes with
145 heights of 5 m to 40 m and thus account for 87% of the total number of occurrences. The
146 remaining 13% take place on slopes with heights of more than 40 m. A high slope normally
147 develops a gentle gradient because of long-term weathering and erosion. By contrast, a low slope
148 generally forms a steep gradient (Zhu et al., 2011), thereby becoming prone to collapses.

149 Sunward slopes are more prone to the development of cracking–sliding failures than shady
150 slopes (**Fig. 4c**). Statistical analysis shows that 69% of the cracking–sliding failures occur on
151 slopes with aspects in the range of 90° to 270°, particularly within 180° to 270° because sunward
152 slopes receive long sunshine hours and soil temperature is relatively high during the day.
153 Therefore, a large temperature difference exists between day and night. Sunward slopes are
154 generally subjected to more weathering than shady slopes, resulting in fractured structures,
155 which are inconducive to slope stability. Furthermore, people usually reside on sunward slopes,
156 and dense human engineering activities exert a large degree of disturbance on the slope body,
157 thereby increasing the occurrence of failures.

158 **4.2 External factors**

159 **1) Rainfall**

160 Rainfall remarkably influences the stability of loess slopes. **In Fig. 6**, the number of loess
161 failures is closely and positively correlated with the average monthly rainfall of the past 15 years.
162 Summer rainfall (July to September) in the study area accounts for approximately 60% of the
163 annual precipitation, and the number of cracking–sliding failures in the same period corresponds
164 to 62% of the total failures. This finding is consistent with that of Gao et al. (2012), who
165 indicated that more than 60% of loess failures happen in Gansu Province in the rainy season.
166 Wei (1995) and Liu et al. (2012) presented a similar conclusion on this phenomenon in Shanxi
167 and Shaanxi, respectively.

168 Rainfall induces loess cracking–sliding failures in three ways, namely, splash erosion, shovel
169 runoff, and seepage. At the beginning of rainfall, soil particles with poor adhesion are separated
170 and broken under the impact of raindrops. When potholes formed by splash erosion are filled
171 with water, a layer of water flow forms and triggers small soil particles to move. Along with the
172 continued rain, this water flow converges into the slope runoff to erode and destroy the slope
173 surface further (Tang et al., 2015). In cases of persistent rainfall, preferential seepage pipes
174 usually develop inside a slope, thereby saturating the soils, reducing the shear strength, and
175 eventually causing cracking–sliding failures.

176 **2) Freezing and thawing**

177 **Fig. 6** shows that cracking–sliding failures occur frequently not only in the rainy season from
178 July to September but also in the winter-to-spring transition from March to April. Soil
179 temperature increases rapidly from a value below 0°C to a value above 0°C. As shown in Fig. 7,
180 soil temperature remains negative, and the frozen depth can reach approximately 1.0 m
181 underground from late November to February in the loess areas in China. At the end of March,
182 the ground temperature begins to increase, and the frozen layer gradually enters the thawing
183 stage. By mid-April, the soil is rapidly heated up to approximately 8 °C.

184 Freezing and thawing mainly promote the occurrence of cracking–sliding failures via two
185 mechanisms: 1) Frost heaving damages the soil structure and reduces soil shear strength. The
186 loess itself contains a considerable number of large pores. Frost heaving further increases the
187 distance between soil particles, reduces the dry density of soil, and loosens the structure, thereby
188 reducing its cohesion and internal friction angle. 2) Thawing causes the loess structure to
189 collapse and reduce its shear strength. Thawed water can dissolve cement, especially calcareous
190 cement, between loess particles, consequently damaging the loess structure and increasing pore
191 water pressure; as a result, the shear strength of the soil decreases (Pang, 1986).

192 **3) Daily temperature fluctuation**

193 Consistent with previous findings (Wei, 1995), our results indicate a relatively high
194 frequency of occurrence of cracking–sliding failures between 10 pm and 4 am (**Fig. 8**). The
195 difference in temperature between day and night in the loess area is more obvious than that in
196 other regions at the same latitude in China (Sun and Zhang, 2011), and variations in air
197 temperature in a day can occasionally reach 30 °C. As shown in **Fig. 9**, the soil at a 50 cm depth
198 shows an average daily temperature difference of approximately 5 °C in summer. Thermal
199 expansion and shrinkage occur during the rapid change in day and night temperatures. Under the
200 cyclic functioning of shrinkage and expansion stresses, a soil structure loosens.

201 **4) Human activity**

202 Loess areas in China have a population of more than 200 million. Human engineering
203 activities frequently occur and mainly involve cutting slopes for buildings, excavation for cave
204 dwellings, and construction of terraced fields and roads. Cutting slopes for buildings causes the
205 side slope to become steep. Unloading-induced tensile fractures are usually produced on the
206 trailing edge of slopes during the rapid adjustment of a stress field within a slope (**Fig. 10a**).
207 When a cave is excavated, roof damage (normally caving) happens because of a local tensile
208 stress concentration if the design of a geometric section of a cave is inappropriate (**Fig. 10b**).
209 Terraced fields change the original path of surface runoff and enhance rainfall infiltration.
210 Together with irrigation, terraced fields increase the water content of loess slopes and increase

211 their phreatic level (Fig. 10c). The majority of traffic lines in the loess area stretch along valleys
212 and bank slopes. Slope cutting and excavation during road construction result in a large number
213 of high and steep side slopes, which provide a suitable environment for failures (Fig. 10d).

214 More than half of the failures are attributed to human engineering activities (Fig. 11). In 2014,
215 9 of 16 failure cases that occurred in Yan'an City were caused by extremely steep slopes for cave
216 dwelling construction, and the 7 other cases were consequences of improper treatment of side
217 slopes for road construction (Lei, 2001). These findings demonstrate that intense human
218 activities likely result in a high probability of loess failures.

219 **5 Conclusions**

220 This study investigates the influencing factors and development patterns of loess cracking–
221 sliding failures in the east of the LPC according to a large collection of field investigation data.
222 The following conclusions are obtained.

223 (1) The influencing factors of cracking–sliding failures are divided into internal and
224 external causes. Internal causes include various features, such as slope geometry, height, gradient,
225 and aspect of loess slopes, whereas external causes comprise rainfall, freezing–thawing cycles,
226 temperature fluctuation, and human engineering activities.

227 (2) Cracking–sliding failure more likely occurs in rectilinear and convex slopes than in
228 concave and stepped slopes. Rectilinear and convex slope gradients are generally steep, stress
229 concentrations are obvious, and slope stability is poor. The stress concentration in concave and
230 stepped slopes is minimized, and stability is fair. Cracking–sliding failure more likely takes place
231 on slopes with gradients of greater than 60° , and the greater the gradient is, the higher the
232 likelihood of failures is. Cracking–sliding failure also tends to occur on slopes with heights of 5
233 m to 40 m. Slopes below 5 m have low internal stress and high stability. Slopes above 40 m are
234 generally gentle with low stress concentration. The dominant aspect of the development of
235 cracking–sliding failure is within 180° to 270° (sunward slopes) because of the evident
236 temperature difference between day and night and the strong weathering.

237 (3) The occurrence of cracking–sliding failure displays a particular time pattern. Within a
238 year, its occurrence coincides with seasonal rainfall. Failures mainly occur in the rainy season, or
239 from July to September. In addition, failures frequently take place from March to April because
240 of freezing and thawing. Within a day, failures happen mostly from 10 pm to 4 am because of the
241 large temperature variation between day and night.

242 (4) The more intense the engineering activities are, the greater the possibility of loess
243 failures is. Human engineering activities in loess areas include cutting slopes for buildings,
244 excavation of cave dwellings, and construction of terraced fields and roads. These engineering
245 activities usually lead to a rapid change in the features and stress field of slopes. Such high and

246 steep side slopes tend to develop unloading-induced tensile fractures, thereby increasing the
247 possibility of loess failures.

248 *Acknowledgments.* This study was supported by the Key Program of National Natural Science
249 Foundation of China (No. 41630640), the Major Program of the National Natural Science
250 Foundation of China (No. 41790445), the 2014 Fund Program for the Scientific Activities of
251 Selected Returned Overseas Professionals in Shanxi Province, Shanxi Scholarship Council of
252 China, Outstanding Innovative Teams of Higher Learning Institutions of Shanxi, Soft-science
253 Fund Project of Science and Technology in Shanxi, Research Project for Young Sanjin
254 Scholarship of Shanxi, Collaborative Innovation Center for Geohazard Process and Prevention at
255 Taiyuan Univ. of Tech., Recruitment Program for Young Professionals of China.

256 **References**

257 Cruden, D. M., and Varnes, D. J.: Landslide types and processes, In: Landslides: investigation
258 and mitigation, Transportation Research Board Special Report., 247, 1996.

259 Gao, H., Zhang, Y. J., and Zhang, X. G.: Factors on geological hazards of loose slope in Lanzhou
260 city, *Gansu Geol.*, 3, 30-36, 2012.

261 Huang, Z., Xu, M., Wang, L., Mi, N., Yu, D., and Li, H.: Shear wave splitting in the southern
262 margin of the Ordos Block north China, *Geophys. Res. Lett.*, 35, 402-411, 2008.

263 Hui, X., Research on relationship between geo-hazard and rainfall in Loess Plateau of Northern
264 Shanxi Province, Ph.D. thesis, Chang'an University, Xi'an, China, 2010.

265 Lei, X. Y.: Geohazards of Loess Plateau and their relation with human activities, *Geol. Press.*,
266 2001.

267 Liu, J., Zhang, P., Lease, R.O., Zheng, D., Wan, J., Wang, W., and Zhang, H.: Eocene onset and
268 late Miocene acceleration of Cenozoic intracontinental extension in the North Qinling range-
269 Weihe graben: Insights from apatite fission track thermochronology, *Tectonophysics*, 584,
270 281-296, 2012.

271 Liu, J. N., Gu, Y., Jin, J., Ni, S. H., and Shen, Y.: Analysis of rainfall, floods and droughts in
272 middle Shanxi in recent years, China, *J. China. Hydrol.*, 2, 51-54, 2013.

273 Lv, M.: The present situation of the loess collapse of geological disasters in Shanxi Province and
274 the water sensitivity analysis, Ph.D. thesis, Taiyuan University of Technology, Taiyuan,
275 China, 2011.

276 Pang, G. L.: A discussion on maximum seasonal frost depth of ground, China, *J. Glaciol.*
277 *Geocryol*, 3, 253-254, 1986.

278 Qian, P.: Study of types for highway drainage system in loess areas in northern Shaanxi Province,
279 Ph.D. thesis, Chang'an University, Xi'an, China, 2011.

280 Qin, L. L., Qi, Q., and Ju, Y. W.: Study on the feature governance research of loess geological
281 disasters in Shanxi Province, China, *Shanxi Archit.*, 6, 58-59, 2015.

282 Qu, Y. X., Zhang, Y. S., and Chen, Q. L.: Preliminary study on loess slumping in the area
283 between northern Shaanxi and western Shanxi – taking the pipeline for transporting gas from
284 west to east in China, *China, J. Eng. Geol.*, 9, 233-240, 2001.

285 Smalley, I., Marković, S. B., and Svirčev, Z.: Loess is [almost totally formed by] the
286 accumulation of dust, *Quaternary International*, 240, 4-11, 2011.

287 Stacey, T. R.: The stress surrounding open-pit mine slope, In: *Planning Open Pit Mine*, 1970.

288 Sprafke, T., and Obrecht, I.: Loess: Rock, sediment or soil - What is missing for its definition,
289 *Quaternary International*, 399, 198-207, 2016.

290 Sun, Z. X., and Zhang, Q.: Analysis of climate characteristics of land surface temperature and
291 energy in the semi-arid region in the Loess Plateau, China, *J. desert Res*, 5, 1302-1308, 2011.

292 Tang, Y. M., Feng, W., and Li, Z. G.: A review of the study of loess slump, China, *Adv. Earth*
293 *Sci.*, 1, 26-36, 2015.

294 Wei, Q. K.: Collapse hazards and its distribution features of time and space in Shaanxi Province,
295 China, *J. Catastrophol.*, 10, 55-59, 1995.

296 Xin, C. L., Yang, G. L., Zhao, Z. P., Sun, X. H., Ma, W. Y., and Li, H. R.: Characteristics,
297 causes and controlling of loess collapses in Beishan mountain of Tianshui city, China, *Bull.*
298 *Soil Water Conserv.*, 33, 120-123, 2013.

299 Yang, W. Z., and Shao, M. A.: Researches of soil moisture in Loess Plateau, *Sci. Press.*, 1995.

300 Zhang, Z.H.: The compilation principle of landscape type map of Chinese Loess Plateau, China,
301 *Hydrogeology and Engineering Geology*, 2, 29-33, 1983.

302 Zhang, Z.H.: Institute of hydrogeology and engineering geology of Chinese Academy of
303 Geological Sciences, China, *Landscape type Map and Instructions of Chinese Loess Plateau*
304 (1:500000), Beijing, Geological Press., 1986.

305 Zhang, Z. Y., Wang S. T., Wang L. S., Huang R. Q., Xu Q., and Tao L. J.: Engineering
306 geological analysis principle, *Geol. Press.*, 2009.

307 Zhang, H.: Study of water migration and strength of the loess under freezing-thawing action,
308 Ph.D. thesis, Xi'an University of Architecture and Technology, Xi'an, China, 2014.

309 Zhu, J. H.: Study on the relationship between slope geometrical morphology and landslide
310 collapse disasters in Yan'an, Ph.D. thesis, Chang'an University, Xi'an, China, 2014

311 Zhu, Y. C., Li, J., and Ren, Z. Y.: Change tendency and relevant analysis about cultivated land
312 and population in Loess Plateau during about 300 years, China, *J. Shaanxi Norm. University*
313 (Natur. Sci. Ed.), 3, 84-89, 2011.

1 **Captions of figures and tables**

2 **Table 1.** Classification of loess slopes.

3 **Figure 1.** The cracking-sliding failure occurred in Shilou County of Shanxi Province on
4 **March 10, 2018 (110°50'48.54"E, 36°59'54.76"N).**

5 **Figure 2.** Geological map of the study area. The red dots denote the cracking–sliding
6 failure cases, and the blue dots indicate the meteorological stations in the study
7 area.

8 **Figure 3.** Statistical analysis results: a) classification of loess slopes in Lishi City, Shanxi
9 Province, China, on the basis of a field survey of 212 loess slopes, indicating
10 that stepped slopes are dominant in the study area. b) Percentage of cracking–
11 sliding failures that occurred in different types of loess slopes across the study
12 area, showing that rectilinear slopes are highly susceptible to loess failures.

13 **Figure 4.** Effect of slope features on cracking–sliding failures.

14 **Figure 5.** Development of tension zones in slopes of different gradients (Stacey, 1970;
15 Zhang et al., 2009).

16 **Figure 6.** Occurrence of cracking–sliding failures mainly in July to September and
17 consistent with the average monthly rainfall.

18 **Figure 7.** Annual variation of temperature (°C) within a shallow zone of a typical loess
19 slope (Yang and Shao, 1995).

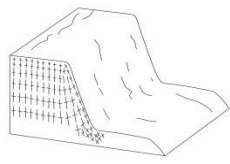
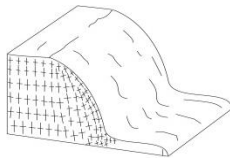
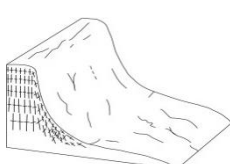
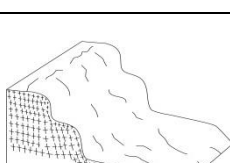
20 **Figure 8.** Temporal distribution of cracking–sliding failures in a day between 10 pm and
21 4 am.

22 **Figure 9.** Daily soil temperature variation in loess areas of China in summer. Data are
23 from the field monitoring during April 2014 to September 2017 in Linxian
24 County, Shanxi, China.

25 **Figure 10.** Typical engineering activities in loess areas in China: a) cut slopes for
26 buildings; b) excavations for cave dwellings; c) terraced fields for farming;
27 and d) cut slopes for highways.

28 **Figure 11.** Role of engineering activities in loess failures: a) Shanxi Province; and b)
29 Huangling County, Shaanxi Province.

30 **Table 1.** Classification of loess slopes.

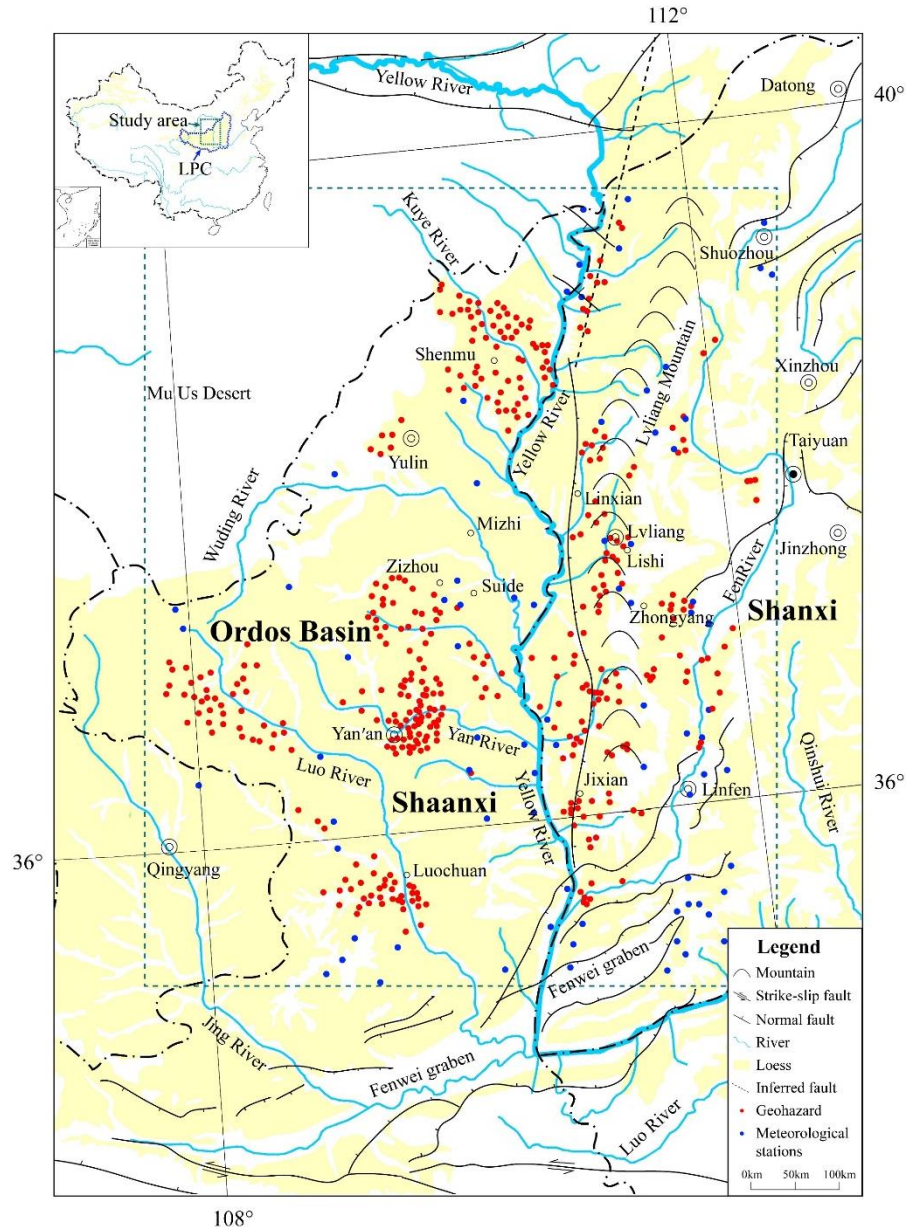
Slope type	Profile	Characteristics	Susceptible ^{#?}
Rectilinear		Slope is straight or nearly straight; slope gradients are fairly large (>55°); stability is low.	Yes
Convex		Gentle at the top and steep at the bottom; convex shoulder; stability is generally poor.	Yes
Concave		Curves inward; gentle toward the toe supporting steep upper slope; more stable than other slopes; stability is fair.	No
Stepped		Stepped with straight faces; average gradient of the overall slope is generally small; stability is good.	No

Note : [#] . susceptibility to cracking–sliding failure.



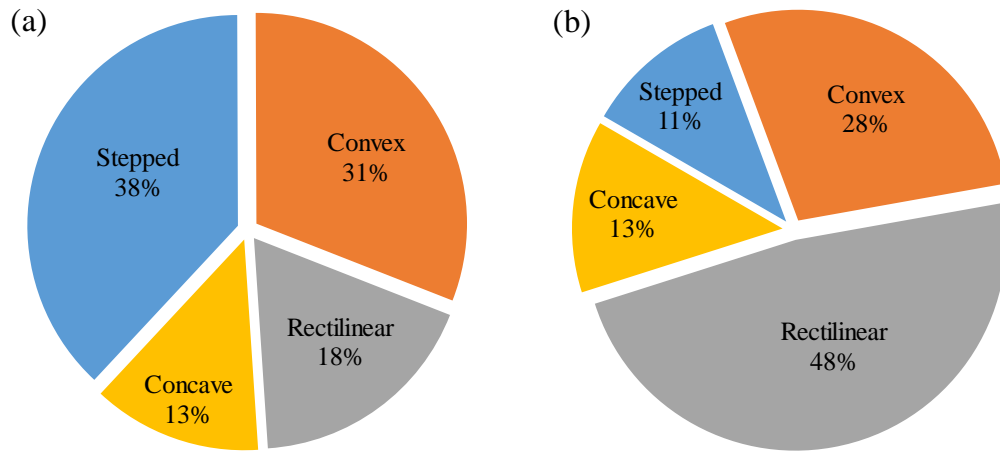
32

33 **Figure 1.** The cracking-sliding failure occurred in Shilou County of Shanxi Province on
34 **March 10, 2018 (110°50'48.54"E, 36°59'54.76"N).**



35

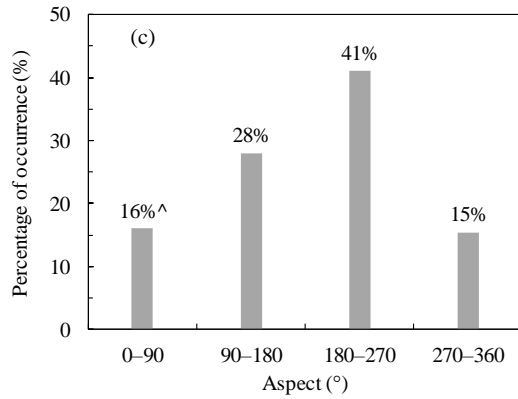
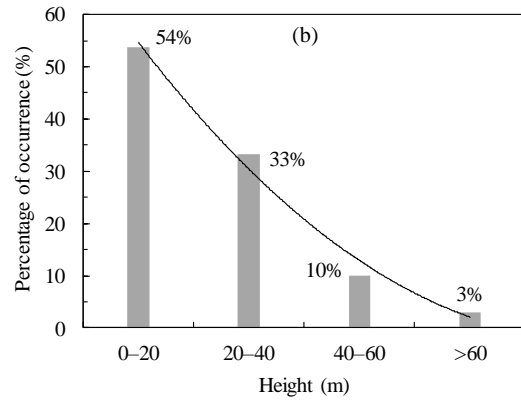
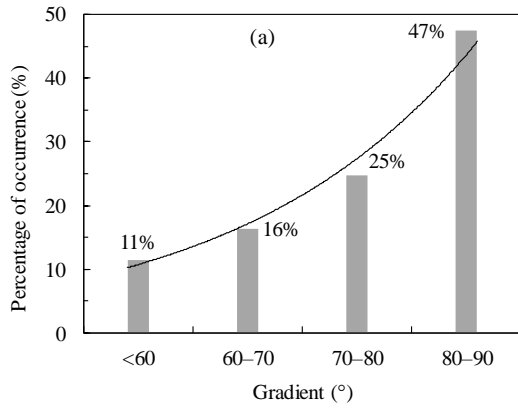
36 **Figure 2.** Geological map of the study area. The red dots denote the cracking–sliding
 37 failure cases, and the blue dots indicate the meteorological stations in the study
 38 area.



39

40 **Figure 3.** Statistical analysis results: a) classification of loess slopes in Lishi City, Shanxi
 41 Province, China, on the basis of a field survey of 212 loess slopes, indicating
 42 that stepped slopes are dominant in the study area. b) Percentage of cracking–
 43 sliding failures that occurred in different types of loess slopes across the study
 44 area, showing that rectilinear slopes are highly susceptible to loess failures.

45



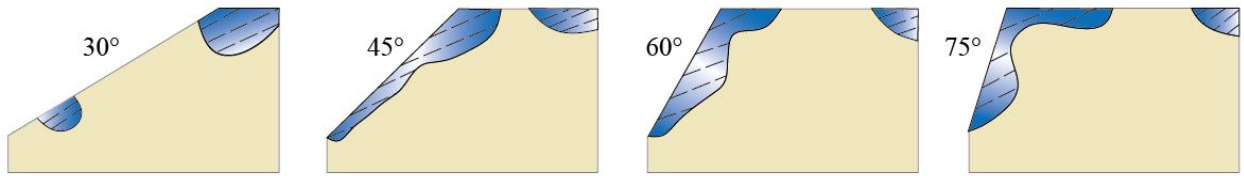
46

47

48 **Figure 4.** Effect of slope features on cracking–sliding failures.

49

50



51

52 **Figure 5.** Development of tension zones in slopes of different gradients (Stacey, 1970; Zhang et
53 al., 2009).

54

55

56

57

58

59

60

61

62

63

64

65

66

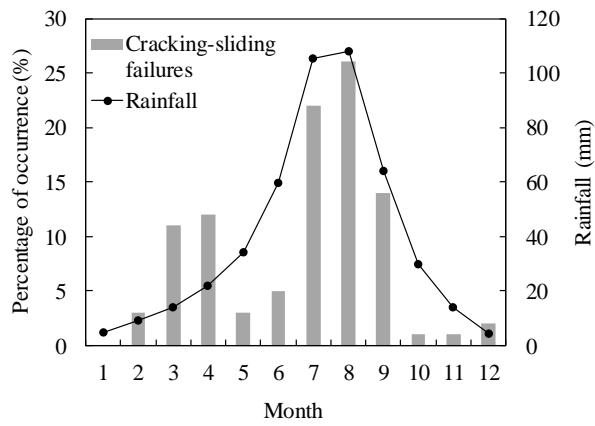


Figure 6. Occurrence of cracking–sliding failures mainly in July to September and consistent with the average monthly rainfall.

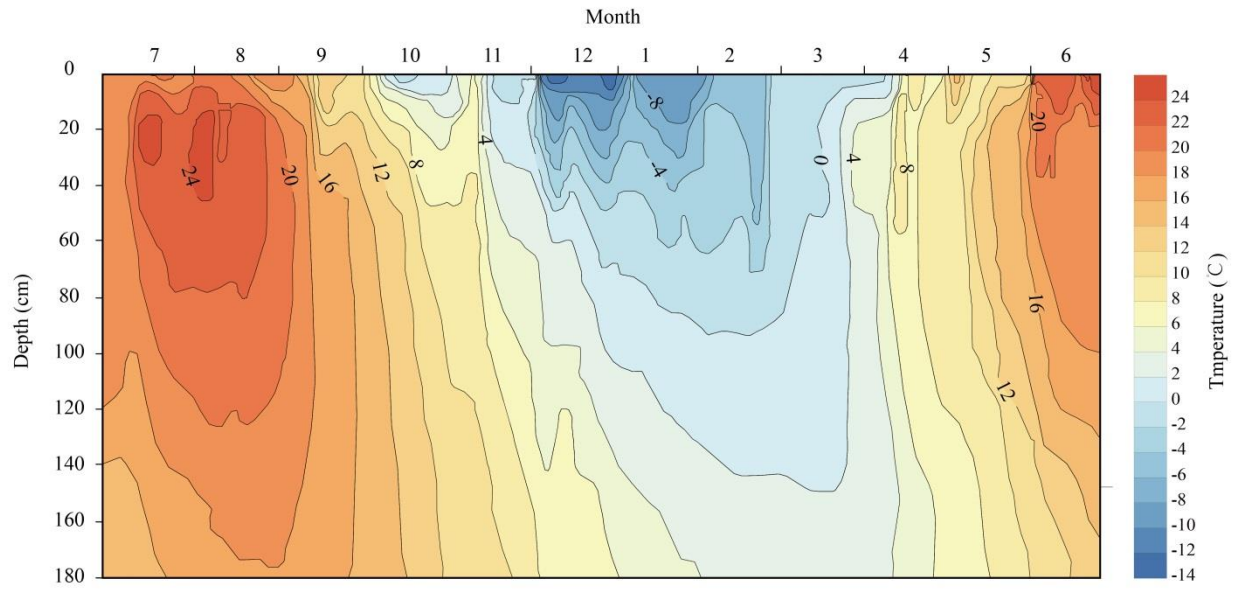


Figure 7. Annual variation of temperature (°C) within a shallow zone of a typical loess slope (Yang and Shao, 1995).

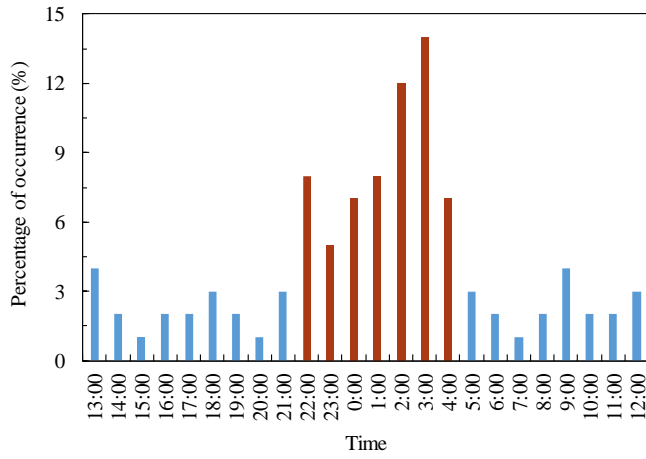


Figure 8. Temporal distribution of cracking–sliding failures in a day between 10 pm and 4 am.

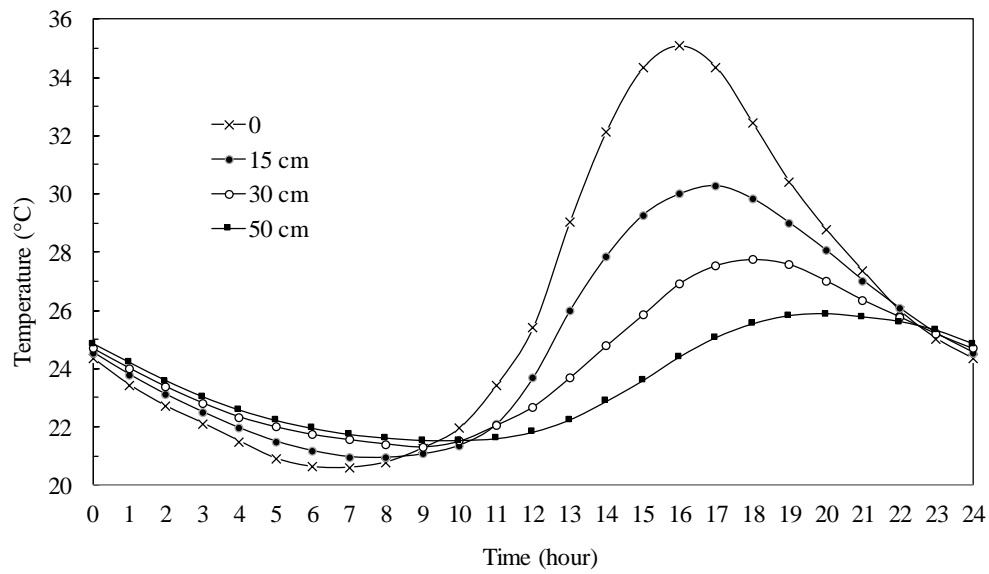


Figure 9. Daily soil temperature variation in loess areas of China in summer. Data are from the field monitoring during April 2014 to September 2017 in Linxian County, Shanxi, China.

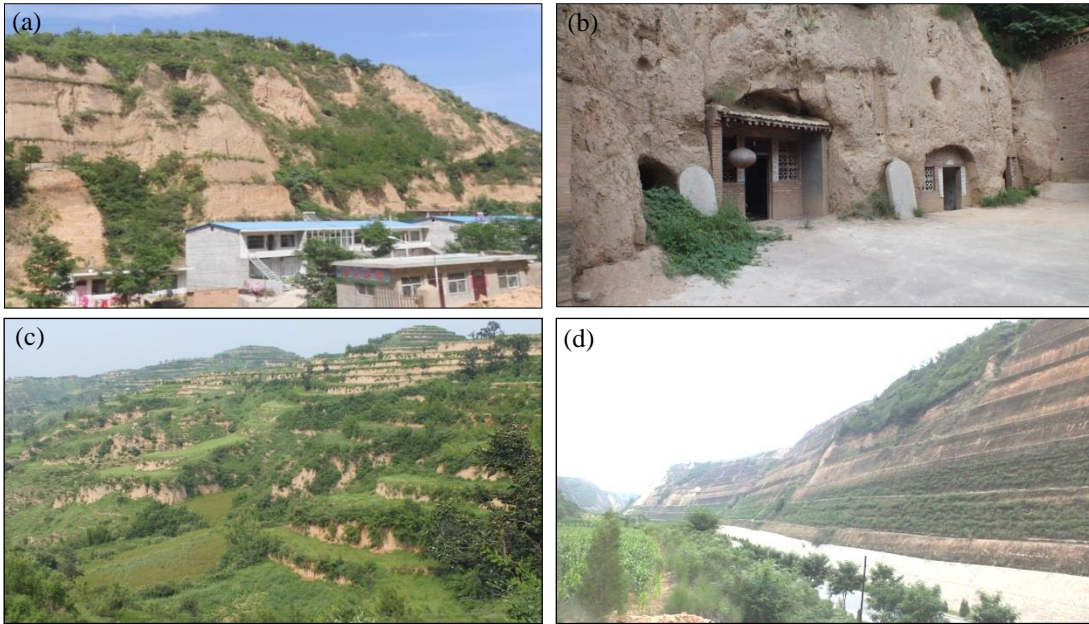


Figure 10. Typical engineering activities in loess areas in China: a) cut slopes for buildings; b) excavations for cave dwellings; c) terraced fields for farming; and d) cut slopes for highways.

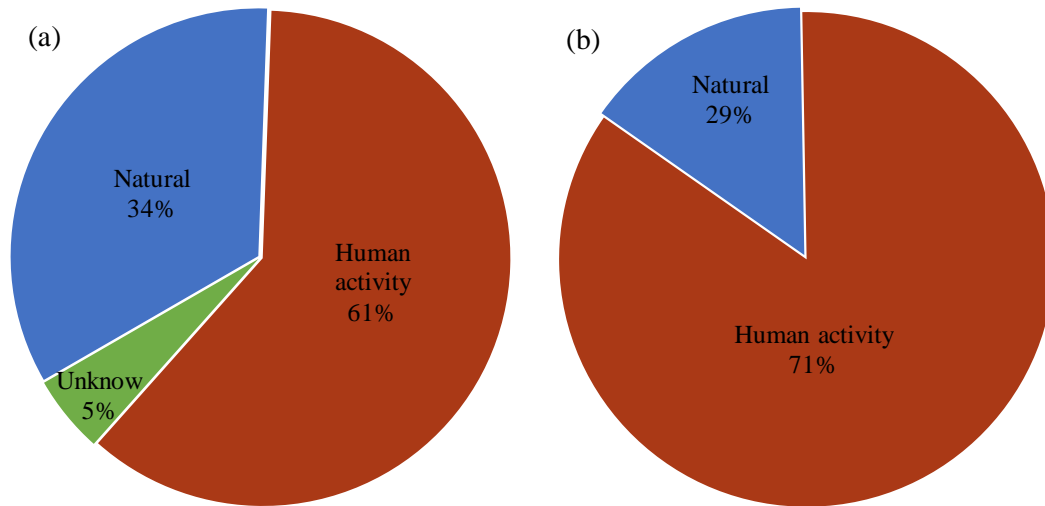


Figure 11. Role of engineering activities in loess failures: a) Shanxi Province; and b) Huangling County, Shaanxi Province.